

Downregulation of *OsPK1*, a cytosolic pyruvate kinase, by T-DNA insertion causes dwarfism and panicle enclosure in rice

Yan Zhang · Wenkai Xiao · Lijuan Luo ·
Jinhuan Pang · Wei Rong · Chaozu He

Received: 1 February 2011 / Accepted: 22 June 2011
© Springer-Verlag 2011

Abstract Pyruvate kinase (PK) catalyzes the final step of glycolysis. There are few reports on the role of PK in rice. Here, we identified a novel rice dwarf mutant, designated as *ospk1*, showing dwarfism, panicle enclosure, reduced seed set, and outgrowth of axillary buds from culm nodes. Sequence analyses of 5'-RACE indicated that a single T-DNA was inserted in the transcriptional regulatory region of *OsPK1* in *ospk1*. Quantitative RT-PCR result showed that *OsPK1* expression was decreased by approximately 90% in *ospk1* compared with that in WT. Enzyme assay and transient expression in protoplasts indicated that *OsPK1* encodes a cytosolic PK (PK_c). Complementation with *OsPK1* demonstrated that *OsPK1* is responsible for the phenotype of *ospk1*. Quantitative RT-PCR and GUS

staining analyses exhibited that *OsPK1* was expressed mainly in leaf mesophyll cells, phloem companion cells in stems, and cortical parenchyma cells in roots. The transcriptions of four other putative enzymes involved in the glycolysis/gluconeogenesis pathway were altered in *ospk1*. The amount of pyruvate is decreased in *ospk1*. We propose that *OsPK1* plays an important role through affecting the glycolytic pathway. The contents of glucose and fructose were markedly accumulated in flag leaf blade and panicle of *ospk1*. The sucrose level in panicle of *ospk1* was decreased by approximately 84%. These findings indicated that both monosaccharide metabolism and sugar transport are altered due to the decreased expression of *OsPK1*. Together, these results provide new insights into the role of PK_c in plant morphological development, especially plant height.

Yan Zhang and Wenkai Xiao contributed equally to this work.

Electronic supplementary material The online version of this article (doi:10.1007/s00425-011-1471-3) contains supplementary material, which is available to authorized users.

Y. Zhang
School of Life Sciences, Tsinghua University,
Beijing 100084, China

Y. Zhang · W. Xiao · C. He (✉)
Shenzhen Laboratory of Super-Hybrid Rice Research,
Graduate School at Shenzhen, Tsinghua University,
Shenzhen 518055, China
e-mail: hecz@im.ac.cn

L. Luo · C. He
Hainan Key Laboratory for Sustainable Utilization of Tropical
Bioresource, Hainan University, Hainan 570228, Haikou, China

J. Pang · W. Rong · C. He
State Key Laboratory of Plant Genomics,
Institute of Microbiology, Chinese Academy of Sciences,
Beijing 100101, China

Keywords Dwarf mutant · Glycolytic pathway · *OsPK1* · Panicle enclosure · Pyruvate kinase · Rice (*Oryza sativa* L.)

Abbreviations

A ₃₄₀	Absorbance at 340 nm
ALT	Alanine transaminase
GC-MS	Gas chromatography-mass spectrometry
Int	Internode
ME	Malic enzyme
OAA	Oxaloacetate
PDH	Pyruvate dehydrogenase
PEP	Phosphoenolpyruvate
PEPC	PEP carboxylase
PEPCK	PEP carboxykinase
PK	Pyruvate kinase
PK _c and PK _p	Cytosolic and plastid PK isozymes, respectively
RACE	Rapid amplification of cDNA ends

RT-PCR	Reverse transcription polymerase chain reaction
TAIL-PCR	Thermal asymmetric interlaced-PCR
TCA	Tricarboxylic acid
TIM	Triosephosphate isomerase
UI	Uppermost internode

Introduction

Pyruvate kinase (PK; ATP:pyruvate 2-*O*-phosphotransferase, EC 2.7.1.40) is a key regulatory enzyme of the glycolytic pathway. It catalyzes the final step of glycolysis, converting ADP and phosphoenolpyruvate (PEP) to ATP and pyruvate by essentially irreversible transphosphorylation. PK requires monovalent (K^+) and divalent cations (Mg^{2+} or Mn^{2+}) for its activity. This enzyme is critical for the control of the metabolic flux through the glycolytic pathway. Moreover, its substrate (PEP) and product (pyruvate) are both involved in a variety of metabolic processes. Thus, PK plays a key role in the cellular metabolic flux.

PK has been purified and characterized from various organisms. Most bacteria and lower eukaryotes have one form of PK, although two forms of PK have been isolated from *Escherichia coli* (Malcovati et al. 1973; Munoz and Ponce 2003). In vertebrates, there are four tissue-specific isozymes: L, R, M1 and M2 (Kayne and Price 1973). In contrast to non-plant PKs, plant PKs are more complicated because of the existence of cytosolic (PK_c) and plastid (PK_p) isozymes (Plaxton 1996). In addition, plant PKs appear to be expressed as tissue-specific isozymes that show substantial differences in their respective physical and kinetic/regulatory characteristics (Plaxton et al. 2002; Plaxton and Podesta 2006).

In plants, PK is subject to a number of regulatory mechanisms, including allosteric control by various metabolite effectors such as Glu and Asp (Hu and Plaxton 1996; Turner and Plaxton 2000; Turner et al. 2005), and phosphorylation and ubiquitination (Tang et al. 2003). Nutrient and hormonal regulation of PK gene expression has been intensively studied in mammalian systems (Yamada and Noguchi 1999), whereas the signals regulating PK expression in plants are poorly known. The differences in the protein accumulation and mRNA expression patterns of PK_c and PK_p in developing tobacco seeds suggest that the tissue-specific and developmental expression of these isoenzymes in tobacco may be controlled by independent transcriptional and post-transcriptional mechanisms (McHugh et al. 1995).

The surprising biochemical complexity and the diverse regulatory mechanisms controlling gene expression and

enzyme activity of higher plant PKs presumably reflect the distinctive metabolic requirements of the respective tissues. In accordance with this point, higher plant PKs have evolved into a family of enzymes to fulfill all of the growth and developmental requirements. Southern blot analyses have revealed that there are at least six PK_c genes in potato (Cole et al. 1992). The *Arabidopsis* genome encodes 14 putative PK isoforms (Arabidopsis Genome Initiative 2000). According to the annotations in GenBank and paralog search results in the KEGG SSDB Database (<http://www.genome.jp/kegg/ssdb/>), the japonica cultivar of rice (*Oryza sativa*) has at least 11 genes that putatively encode different PK polypeptides.

The role of PK in plant growth and development is an interesting subject, because growth and development are closely linked to agricultural economy. In *Arabidopsis* seeds, PK_p was shown to be involved in fatty acid biosynthesis (Andre et al. 2007; Baud et al. 2007). The impacts of modified PK_c levels on plant metabolism have also been studied. Transgenic tobacco lacking leaf PK_c showed altered growth, carbon partitioning and dark respiration (Knowles et al. 1998; Grodzinski et al. 1999), which demonstrated the importance of this enzyme in the control and integration of plant carbon and energy metabolisms. A recent study on the effect of decreased PK_c on potato tuber metabolism showed that PK_c has a crucial role in the regulation of levels of pyruvate and alternative oxidase in heterotrophic plant tissue (Oliver et al. 2008). However, the role of PK_c in rice has not yet been reported.

Plant height is an important agronomic trait for grain production of rice, and numerous dwarf mutants have been investigated in detail in other studies. In this study, we identified a novel rice dwarf mutant, designated as *ospk1*, from our T-DNA tagged population. The present study is focusing on the gene expression effects of *OsPK1*. The main impacts of decreased transcription levels of *OsPK1*, which encodes a tissue-specific PK_c , were reductions in plant height and viable seed number per panicle, both of which are important agronomic traits. Our results indicate that *OsPK1* plays an important role in the glycolytic pathway, and therefore *OsPK1* is critical for the morphological development of rice.

Materials and methods

Plant materials

Rice (*Oryza sativa*) japonica cultivar Nipponbare was used as WT in this study. The mutant *ospk1*, in the Nipponbare background, was screened from a T-DNA tagged population (Sha et al. 2004). The mutant seeds were supplied by Chaozu He (State Key Laboratory of Plant Genomics,

Institute of Microbiology, Chinese Academy of Sciences). Rice plants were grown in an experimental field in natural growing seasons or in a light incubator under a 14 h light/10 h dark photoperiod (30/26°C). Seedlings within 1 week were obtained by accelerating germination as follows: decorticated rice seeds were placed on filter paper soaked in sterilized water, germinated in darkness at room temperature for 3 days, and then transferred into the light incubator.

Scanning electron microscopy (SEM) analysis

To compare the internode parenchyma cell length of *ospk1* with that of WT, longitudinal sections of the elongated zone of the UI were fixed in 2.5% glutaraldehyde, dehydrated through an ethanol series, and dried with a critical point drier. The dried samples were mounted on aluminum stubs, coated with gold, and then visualized using a QUANTA 200 environmental scanning electron microscope (FEI) at 10 kV.

Identification of T-DNA insertion

Genomic DNA flanking the right border of the T-DNA insertion in *ospk1* was obtained by thermal asymmetric interlaced-PCR (TAIL-PCR) as described previously (Liu et al. 1995; Sha et al. 2004). In Fig. 2a, b, LP1, LP2, RP1 and RP2 refer to specific primers of rice genomic DNA at the T-DNA left or right flank, respectively, and LB and RB refer to the T-DNA left and right border primers, respectively. Confirmation of the T-DNA insertion site and genotyping analyses of *ospk1* were carried out using the primers LP1 (forward, 5'-TACAATAACGAAGACGCC-3') and RP1 (reverse, 5'-GTTGCCATTAGACAATAA-3') to amplify the interrupted fragment. LP2 (forward, 5'-ATCCAATAACAATAACGAAGAC-3') and LB (reverse, 5'-TCCTAAAACCAAAATCCA-3') were used to confirm the sequence flanking the left border of the T-DNA insertion. RB (forward, 5'-TgATTAgAgTCCCgCAATT-3') and RP2 (reverse, 5'-CTACTATACACCTCCgTTT-3') were used to confirm the right flank.

RACE reactions

Total RNA was isolated from axillary bud tissue using TRIzol reagent (Invitrogen). The 5'-Full RACE kit and 3'-Full RACE Core Set Ver. 2.0 (TaKaRa) were used for 5'- and 3'-rapid amplification of cDNA ends (RACE), respectively, according to the manufacturer's manuals. The *OsPK1*-specific primers were designed based on the Os11g0148500 mRNA sequence (GenBank accession number NM_001072281) and used to amplify 5'- and

3'-RACE-ready cDNAs. The *OsPK1*-specific primers used for PCR amplification were as follows: 5'-RACE-GSP1, 5'-CGGATCAGATCGGGAGGTAGA-3', 5'-RACE-GSP2, 5'-AGCGTCAGCGGCTGCTCGAT-3'; 3'-RACE-GSP, 5'-TTGATGATACTACGGCAAGT-3'. The RACE products were then cloned into the vector pGEM-T (Promega) for sequencing. For 5'-RACE confirmation, PCR was performed using the primers 5'-ATATGCTGCGATTCCACGTT-3' (forward) and 5'-CAGGAGGAGATGGTGTGCG-3' (reverse).

Quantitative and semi-quantitative RT-PCR

Total RNA was extracted using TRIzol reagent (Invitrogen). RNA quality was assessed by agarose gel electrophoresis prior to DNase I (Invitrogen) digestion. First-strand cDNA was synthesized from 5 µg total RNA using the SuperScript III First-Strand Synthesis System (Invitrogen).

Real-time PCR experiments were performed using SYBR *Premix ExTaq* (Perfect Real Time; TaKaRa) and the DNA Engine Opticon 2 Continuous Fluorescence Detector (MJ Research) according to the manufacturer's protocols. The rice *Actin1* gene was used as an internal control in the analysis (primer pair: forward, 5'-TGCTATGTACGTCGCATCCAG-3' and reverse, 5'-AATGAGTAACCACGCTCCGTCA-3'; Dai et al. 2007). Fluorescence intensity was measured at 76°C. PCR was performed using the following primer sets: *OsPK1* (Figs. 2 and 5), forward, 5'-TGCCTC GATTGATTGATT-3', reverse, 5'-CAGGAGGAGATGGTGTGCG-3'; *OsPK1* (Fig. 3), forward, 5'-TCGTGGGGACGCTGGGTCCC-3', reverse, 5'-TCACCACCTGCAACTCCG-3'; Os12g0145700, forward, 5'-ACCGCCCGCTTAGGTTT-3', reverse, 5'-AATCGGGCCACCGACATG-3'; Os09g0535000, forward, 5'-CAAACCTGGGCGGATGTAG-3', reverse, 5'-AACAAGGAAGCCGTCAAT-3'; Os06g0256500, forward, 5'-CGCTAATCTGCGACACCG-3', reverse, 5'-TTGAGCTTTGCCGCCTCT-3'; Os04g0119400, forward, 5'-ACGTTCTGTCATGGCTGAG-3', reverse, 5'-CCAGGGTTACATCAAGTCC-3'; Os01g0866400, forward, 5'-GTGAATGAAGGGAATGCG-3', reverse, 5'-GCC TGCTCCATCAGGAAT-3'.

Semi-quantitative RT-PCR analysis of genes related to pyruvate/PEP metabolism was performed using the following primer sets: Os01g0188400 (*ME6*), forward, 5'-GTTGTCAGGGAATGGGTAT-3', reverse, 5'-GCAAA TCAAATGCGTTGT-3'; Os10g0204400 (*PEPCK*), forward, 5'-ATCAAATATGAGAAAGGGTC-3', reverse, 5'-AAGGGAGTTCAAGTAGTCAA-3'; Os02g0244700 (*PEPC-1*), forward, 5'-GAGGTGGTCCCAGTCATC-3', reverse, 5'-TATTCAACAAACCGTGGC-3'; Os01g0208700 (*PEPC-2*), forward, 5'-CCGGAAGTCTCAAGGAA-3', reverse, 5'-ACAGCGATCGGTAGCACA-3'; Os10g0390500 (*ALT-1*), forward, 5'-TTTGTACTCAGCCTCCAT-3',

reverse, 5'-ACACCTCATCAGCCAGAA-3'; Os07g0108300 (ALT-2), forward, 5'-ACTGGGGACTTGACTTCG-3', reverse, 5'-CAGAACCTTTCTAGCACTTA-3'. Genes encoding putative PK were analyzed using the following primer sets: Os12g0145700, *OsPK1* (Figs. 2 and 5) and *Actin1*, mentioned above; Os07g0181000, forward, 5'-AGGAGATAATCCGTGCTT-3', reverse, 5'-TTGCTGACTCACCTGAA A-3'; Os10g0571200, forward, 5'-GTACAATGCGAAGAA TACTGA-3', reverse, 5'-TCCTCCATCCACCAACAG-3'; Os03g0672300, forward, 5'-GGGCTTCCTACATTGTCA-3', reverse, 5'-AGATGCCTCTATGATGTCTTTA-3'; Os04g0677500, forward, 5'-TCTGTGCTTTGTCCGTA-3', reverse, 5'-AGTCACAACAGGCTTTCC-3'.

Each analysis was biologically repeated twice, and representative results are shown. Each cDNA template was assayed in triplicate.

Vector construction and rice transformation

For complementation of the *ospk1* mutant, PCR was performed using primer pairs GF1 (5'-TTCTAGAGTGCCAGACACATCTGTTCTAGAAGC-3') and GR1 (5'-TAACTGTGCGCACATCTTC-3') for the 3003-bp genomic fragment, and GF2 (5'-GAGTATGCACTGATTCCAGG-3') and GR2 (5'-TGGTACCGAAGTCGCCGACCACAA CAG-3') for the second fragment containing 2913 bp. The two fragments were cloned into pGEM-T (Promega) and verified by sequencing. The overlap of the two fragments contained a *SacI* site, which was used for ligation of the two parts. Then, a 5812-bp genomic fragment containing the entire *OsPK1* coding sequence, 1544 bp of the 5' upstream region, and 599 bp of the 3' downstream region was cloned into the *XbaI/KpnI* sites of pCAMBIA2301. The full-length CDS of *OsPK1* was amplified by RT-PCR using primers CF (5'-CAAGATCTATGCATTCGACGAA TCTGC-3') and CR (5'-CTGGTGACCTAATCGTCCAGCTCAATGATC-3'). After sequence verification, the fragment was introduced into the pCAMBIA1301 vector by digesting with *BglIII/BstEII*. The CDS of *hptII* in pCAMBIA1301 was replaced with the CDS of *nptII* in pCAMBIA2301 by *XhoI* digestion, resulting in another T-DNA construct to rescue the phenotype of *ospk1*. Each construct was transformed into the *ospk1* mutant via an *Agrobacterium*-mediated method as described previously with minor modifications (Hiei et al. 1994). Transformants were selected on medium containing 150 mg l⁻¹ G418.

For promoter analysis, a fragment containing 1,544 bp upstream of the ATG start codon and the first 24 bp of the CDS was amplified using primers GF1 and PR (5'-CTCCATGGCAGCAGCAGATTCTCGAATGCAT-3'), and was inserted in front of the *GUS* gene in pCAMBIA1301 by digesting with *XbaI/NcoI*. The resulting

PRO_{OsPK1}:GUS construct was introduced into WT by *Agrobacterium*-mediated transformation.

Subcellular localization

To determine the subcellular localization of *OsPK1*, we constructed *CaMV35S:OsPK1-GFP*. The CDS of *OsPK1* was amplified by RT-PCR with the primer pair (forward, 5'-CATCTAGAATGCATTCGACGAATCTGC-3' and reverse, 5'-CTGGATCCAATCGTCCAGCTCAATGATC-3'). The amplified product was cloned into vector pBI221-G by digesting with *XbaI/BamHI*. Protoplast preparation and transfection were carried out as described previously with some minor modifications (Li et al. 2005). Protoplasts were transfected with either the *CaMV35S:OsPK1-GFP* construct or the empty vector and incubated in W5 medium [154 mM NaCl, 125 mM CaCl₂, 5 mM KCl, and 2 mM MES (pH 5.7)]. After incubation overnight in the dark, GFP signals and chlorophyll autofluorescence were observed under a Zeiss LSM 510 Meta confocal microscope.

GUS staining

Histochemical staining of GUS activity was performed using a standard method. Plant tissue was incubated in X-Gluc staining solution [1 mM 5-bromo-4-chloro-3-indoyl- β -D-glucuronide, 100 mM sodium phosphate, pH 7.0, 10 mM EDTA, 0.1% Triton X-100, 2.5 mM K₄Fe(CN)₆ and 2.5 mM K₃Fe(CN)₆] at 37°C for 12–15 h. After incubation, tissue was decolorized in 70% ethanol.

For microscopic observations, leaf blades, internodes and roots were immersed in fixing solution [50% ethanol, 5% glacial acetic acid, 3.7% formaldehyde] after GUS staining, and then dehydrated in a gradient ethanol series. The samples were embedded in paraffin wax (Sigma) after vitrification. Microtome sections (10 μ m) were mounted onto poly-L-lysine coated slides (Sigma) and dewaxed with xylene. The sections were mounted using neutral balsam and observed and photographed under an Olympus BX51 microscope.

In vitro expression and enzyme assay

The full-length CDS of *OsPK1* was amplified via RT-PCR using primers 5'-GGAATTCGATGCATTCGACGAATCTGCTGC-3' (forward) and 5'-CCTCGAGATCGTCCAGCTCAATGATC-3' (reverse), and cloned into the expression vector pET-23b(+) (Novagen), resulting in the pET-23b(+)-*OsPK1* construct. Expression of the His-tagged protein in the *E. coli* expression strain BL21(DE3) was induced with 0.2 mM isopropyl- β -D-thiogalactoside at 28°C for 4 h. The fusion protein was purified using

Ni-NTA magnetic agarose beads (Qiagen) under native conditions according to the manufacturer's instructions.

Pyruvate kinase activity was assayed by coupling the production of pyruvate to the conversion of NADH to NAD⁺ as described previously with minor modifications (Andre et al. 2007). Reactions were initiated by the addition of enzyme, and the assay mixture was incubated at 25°C for 5 min. Absorbance at 340 nm was monitored using a DU 800 UV/Vis Spectrophotometer (Beckman Coulter). Standard PK_c reaction mixtures contained 50 mM 3-(*N*-morpholino)propanesulfonic acid (MOPS)-KOH, pH 7.0, 5% polyethylene glycol 8000, 50 mM KCl, 15 mM MgCl₂, 1 mM DTT, 2 mM PEP, 1 mM ADP, 0.2 mM NADH, and 2 units ml⁻¹ lactate dehydrogenase from rabbit muscle (Sigma-Aldrich). To assay enzymatic activity, 100 pmol purified protein was used per reaction. A reaction containing 2.5 Units ml⁻¹ pyruvate kinase from rabbit muscle (Sigma-Aldrich) served as the positive control.

Determination of pyruvate and PEP contents

Metabolites from 100 mg leaf sample were extracted with chloroform/water/methanol as described previously (Hausler et al. 2000). The aqueous phase of the extracts was filtered and dried overnight in a vacuum concentrator. Residues were redissolved and subjected to HPLC for measurement of pyruvate and PEP. Reversed phase HPLC was performed on Agilent 1200 equipment. A Supelcosil LC-18-Tcolumn (3 μm, 4.6 × 150 mm) was eluted with 0.5% (NH₄)₂HPO₄-H₃PO₄ (pH 2.5, Solvent A) and methanol in a linear gradient (0–8%, Solvent B) at a flow rate of 0.5 ml min⁻¹, monitoring at 214 nm by diode-array detector. Pyruvic acid (BBI) and PEP-K (Sigma) were used as standard samples.

Determination of sugar contents

Glucose, fructose, galactose, and sucrose in flag leaf blade, internode and panicle of WT and mutant plants were extracted with 80% methanol and quantified by GC-MS analysis as previously described (Tan et al. 2010).

Results

Characterization of the *ospk1* mutant

To identify mutants showing morphological alterations, we screened our T-DNA insertion lines of rice (Sha et al. 2004). *ospk1* was selected for further analysis because of its unique phenotypes, including dwarfism, panicle enclosure, reduced seed set, and the outgrowth of axillary buds

from culm nodes (Fig. 1a–e). The segregation ratio was 3.13:1 (normal:dwarf = 25:8) in the progeny of the self-pollinated T₀ generation, a ratio close to 3:1 ($\chi^2 = 0.01$, $P > 0.9$). Southern blotting analysis revealed that a single-copy T-DNA was inserted in *ospk1* (Sha et al. 2004). These results suggested that *ospk1* is a single recessive mutant.

Compared with that of wild type (WT), the germination of *ospk1* was delayed by nearly 2 days (Fig. S1a). Both the shoot and root of young *ospk1* seedlings were shorter than those of WT (Fig. S1b,c). After internode elongation, *ospk1* showed a dwarf phenotype with shorter leaves (Fig. 1a; Table 1). After the heading stage, panicle enclosure was a typical phenotype of *ospk1* (Fig. 1b). Compared with WT, *ospk1* showed marked reductions in seed number per panicle and seed set (Fig. 1c; Table 1). *ospk1* showed approximately 29% seed set, compared with 93% in WT. The panicles of *ospk1* were shorter than those of WT (Fig. 1c; Table 1).

All internodes of *ospk1* were shorter than those of WT (Fig. S1d). However, the uppermost internode (UI) of *ospk1* was reduced obviously (Fig. 1f). Thus, the dwarfism of *ospk1* is an 'sh' type, based on the classification of dwarf mutants (Yamamuro et al. 2000). As shown in electron micrographs of longitudinal sections of the elongated zone of the UI, the parenchyma cell length was decreased in *ospk1* (Fig. 1g).

The tillering process continues throughout the life of the plant (Li et al. 2003). In *ospk1*, the axillary buds were released from the dormant stage and grew out from culm nodes in the productive phase, whereas those of WT remained dormant (Fig. 1d, e). In general, three or four side shoots developed from axillary buds of a single culm in *ospk1*. Other morphological abnormalities in *ospk1* plants included thin culms, shrunken grains, and slightly increased tiller number (Fig. 1c–e; Table 1).

To identify which gene was disrupted in the mutant, we used TAIL-PCR to obtain the genomic sequences flanking the T-DNA insert junctions in *ospk1* (Liu et al. 1995; Sha et al. 2004). Analysis of the flanking sequences revealed that a T-DNA integration occurred at nucleotide position 349 bp upstream of the ATG start codon of Os11g0148500, which was accompanied by a 29-bp deletion of rice genomic DNA (Fig. 2a). The insertion site was further confirmed by PCR amplification with T-DNA left border, right border, and genome-specific primers (Fig. 2b). Based on the *O. sativa* ssp. *japonica* genome sequence, there is a single copy of the Os11g0148500 gene. We named the gene *OsPK1*.

Sequence analyses of 5'- and 3'-RACE products indicated that the full-length *OsPK1* cDNA is 2,077-bp long, with an ORF of 1,584 bp, a 229-bp 5'-untranslated region, and a 264-bp 3'-untranslated region. Sequence comparison between the genomic DNA and cDNA

Fig. 1 Characteristics of *ospk1* mutant. **a** Gross morphology of WT and *ospk1* at the productive phase. **b** Typical panicle enclosure phenotype observed in *ospk1*. **c** Panicles of WT and *ospk1*. Panicles of *ospk1* contained more empty and shrunken grains than those of WT. **d, e** Outgrowth of axillary buds from culm nodes of *ospk1* at the productive phase. Black arrow indicates new shoot with panicle developed from axillary bud. Leaves have been removed to show internodes and developing axillary buds. **f** Percentage contribution of each internode to the total internode length. 1–5, internodes numbered from top to bottom. **g** Electron micrographs of longitudinal sections of elongated zone of the UI. Bars 100 μm

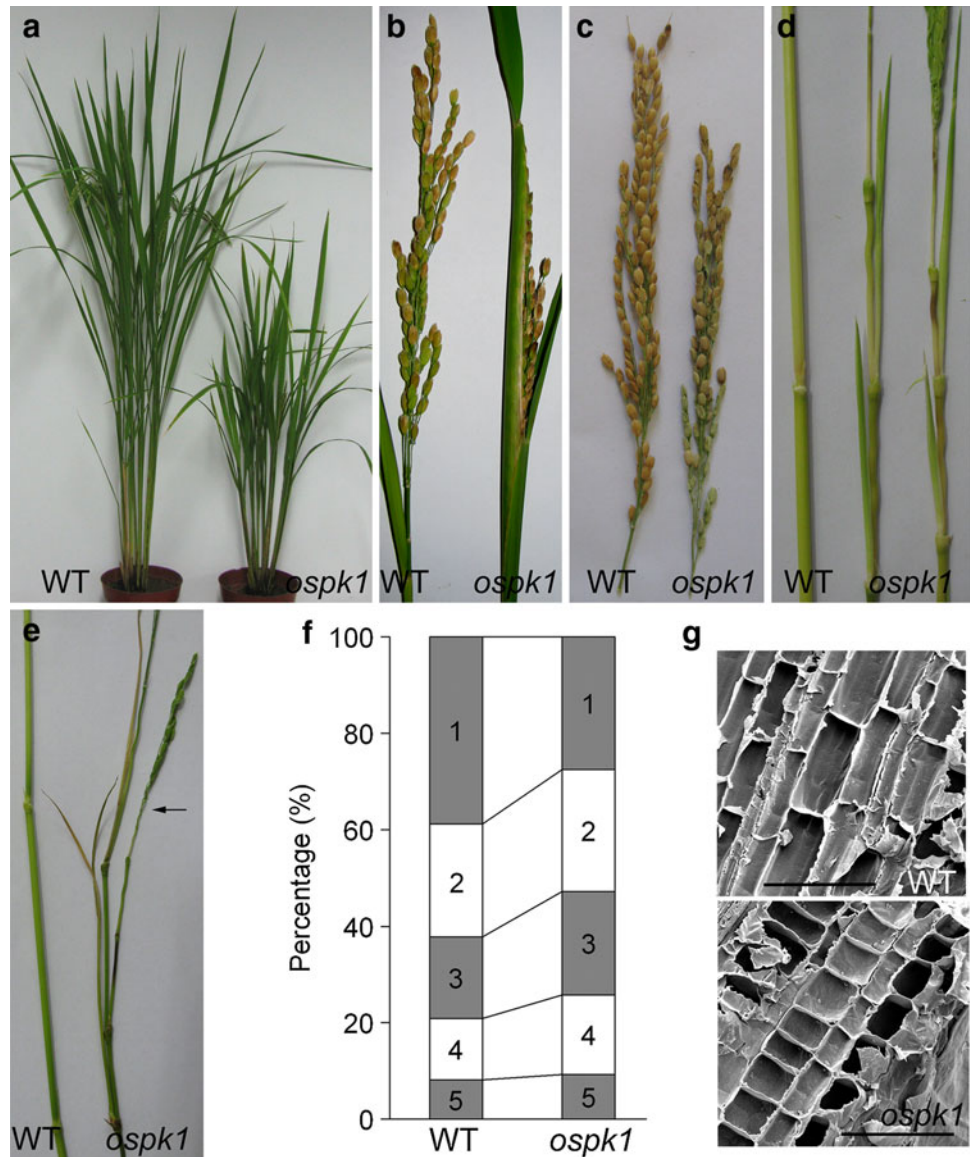


Table 1 Statistical analysis of agronomic traits

Agronomic traits	WT	<i>ospk1</i>	<i>ospk1</i> -gc	<i>ospk1</i> -cc
Height (cm)	99.2 ± 3.2	43.2 ± 4.4	ND	ND
Tiller number	8.3 ± 2.1	10.5 ± 1.9	ND	ND
Panicle length (cm)	20.3 ± 1.3	16.7 ± 1.5	18.7 ± 0.8	20.7 ± 1.2
Seed set (%)	93.2 ± 4.0	29.3 ± 13.2	84.3 ± 3.8	86.2 ± 6.9
Viable seeds per panicle	94.2 ± 12.2	26.6 ± 11.6	79.3 ± 6.4	91.3 ± 10.3

Values shown are average ± SD (*n* = 15 plants or panicles)
 ND not determined

revealed that *OsPK1* consists of 16 exons (Fig. 2a). The mRNA expression levels of *OsPK1* in WT and *ospk1* were quantified using real-time RT-PCR. Compared with that in WT, expression of *OsPK1* was decreased by approximately 90% in the root, leaf, internode and panicle of *ospk1* (Fig. 2c). Thus, the T-DNA insertion site is not in the 5'-UTR, but in the transcriptional regulatory region of *OsPK1*.

To confirm that the *OsPK1* mutation is responsible for the *ospk1* phenotype, a 5,812-bp genomic fragment containing the entire *OsPK1* coding sequence, 1,544 bp of the 5' upstream region, and 599 bp of the 3' downstream region was amplified by PCR and cloned into pCAM-BIA2301. The complementation construct was then transformed into the *ospk1* mutant. A T-DNA construct containing a CaMV 35S-driven full-length CDS of *OsPK1*

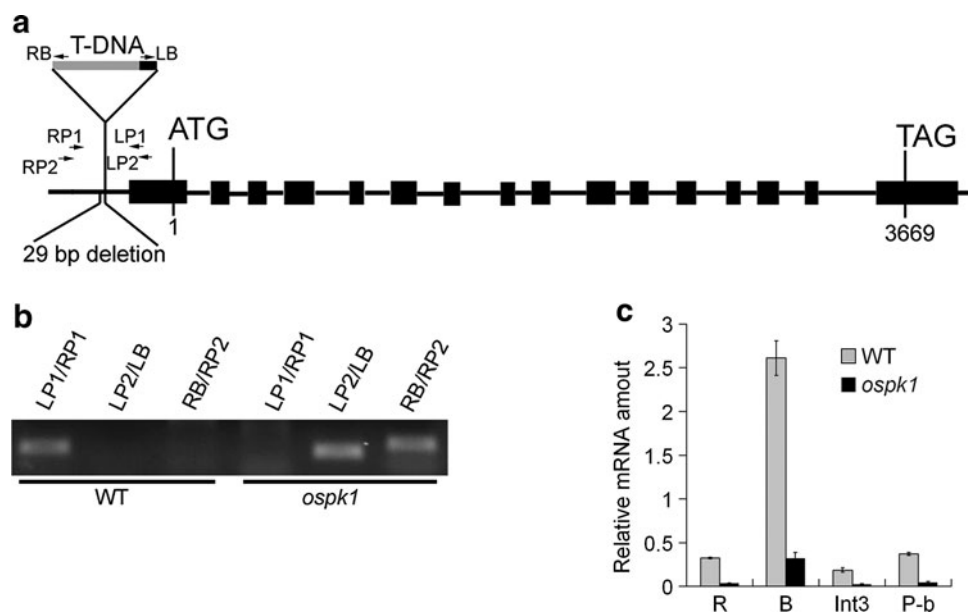


Fig. 2 Identification of the T-DNA mutant *ospk1*. **a** Gene structure of *OsPK1* and location of T-DNA insertion. Black box on T-DNA shows left border. *LP1*, *RP1*, *LP2*, *LB*, *RB* and *RP2* show locations of primers used for genotyping in **b**. ATG, start codon; TAG, stop codon. The 29-bp deletion was from nt -121 to -149 upstream of the transcription initiation site. **b** PCR-based genotyping of *ospk1*. *LP1*, *LP2*, *RP1*, and *RP2* denote specific primers of rice genomic DNA at

left or right flank of T-DNA. *LB* and *RB* denote T-DNA left and right border primers, respectively. **c** Quantitative RT-PCR analysis showing differential expression of *OsPK1* in WT and *ospk1*. Transcription level was normalized to that of rice *Actin1* gene in different organs. *R* young root, *B* leaf blade of 1-month-old seedling, *Int3* the third internode counted from top, *P-b* young panicle at booting stage

was also used to rescue the phenotype of *ospk1*. Whether the introduced fragment was genomic DNA or CDS of *OsPK1*, the phenotypes of these transgenic plants, including plant height and seed set, totally reverted to that of WT, and panicle enclosure was eliminated (Fig. 3a, b; Table 1). The seed germination was also restored (Fig. 3c). The *OsPK1* transcription levels in mature leaves of complementation transgenic plants are elevated and close to that in WT (Fig. 3d). The positive complementation transgenic lines were identified by PCR-based genotyping analyses (Fig. 3e). These results indicated that a T-DNA insertion into the transcriptional regulatory region of *OsPK1* is responsible for the phenotype of *ospk1*.

Subcellular localization of OsPK1

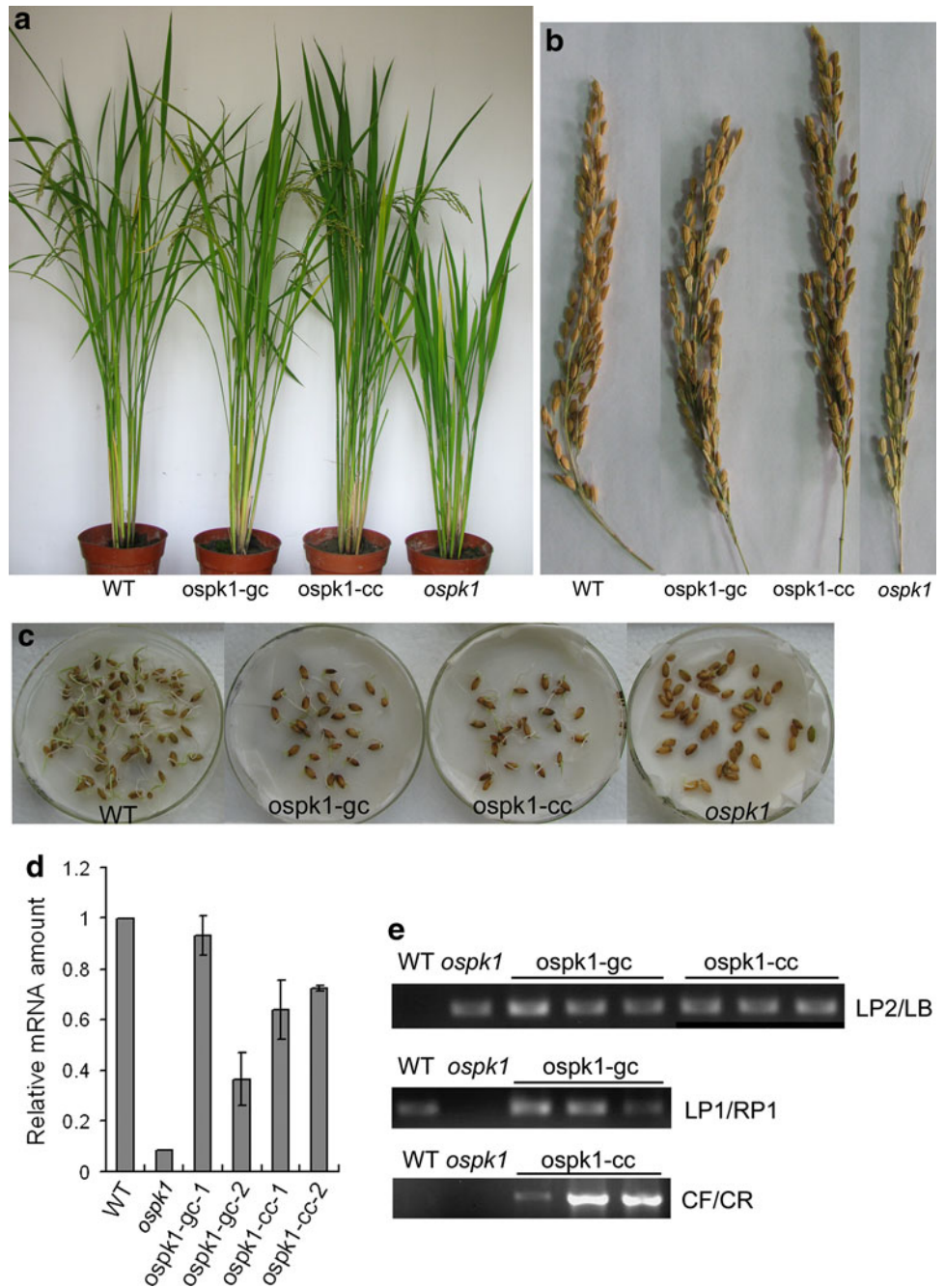
The OsPK1 protein was predicted to be cytoplasmic by PA-SUB Server v2.5 (<http://pasub.cs.ualberta.ca:8080/pa/Subcellular>) and WoLF PSORT (<http://wolffpsort.org/>). To verify this prediction, a OsPK1-GFP fusion protein driven by the CaMV 35S promoter was expressed transiently in *Arabidopsis* mesophyll protoplasts. Fluorescence of cytoplasmic strands was clearly visible, but the GFP signal was barely visible in the corresponding chlorophyll autofluorescence region (Fig. 4). These results suggest that OsPK1 is a cytosolic protein.

Expression pattern of *OsPK1*

Organ and tissue specificity of *OsPK1* gene expression were examined by quantitative real-time RT-PCR (Fig. 5a). The highest level of *OsPK1* expression was in leaves, followed (in decreasing order) by the coleoptile, the panicle at the heading stage, and the young root. There were very low levels of *OsPK1* expression in the shoot apex and internodes. It is interesting to note that transcript level of *OsPK1* in the panicle at the heading stage was nearly double that in the panicle at the booting stage. We also found that the mRNA level of Os12g0145700, which has 96.4% amino acid sequence identity with *OsPK1*, was much lower than that of *OsPK1* (Fig. 5a).

To further investigate the pattern of *OsPK1* expression, particularly its cellular expression pattern, we amplified approximately 1.5 kb upstream of the ATG start codon of Os11g0148500 and introduced the amplified fragment into the pCambia1301 vector, resulting in the *PRO_{OsPK1}:GUS* construct. The expression pattern was clearly visible in transgenic rice plants harboring the *PRO_{OsPK1}:GUS* construct (Fig. 5b–k). In young seedlings, GUS staining was strongest in the coleoptile and the maturation zone of the radicle, fainter in the elongation zone, and barely detectable in the meristematic zone of the radicle (Fig. 5b). Higher levels of GUS expression were observed in adventitious roots than in the root-hair zone of primary

Fig. 3 Phenotypic complementation by introduction of *OsPK1*. **a–c** Gross morphology at the productive phase, panicle and seed germination of WT, transgenic and mutant plants, respectively. *ospk1-gc* and *ospk1-cc* denote plants transformed with genomic DNA and a CaMV 35S-driven full-length CDS of *OsPK1*, respectively. **d** The transcription levels of *OsPK1* in mature leaves. The level in WT is set as 1. **e** PCR-based genotyping analysis of WT, *ospk1*, *ospk1-gc*, and *ospk1-cc*. *LP2*, *LB*, *LP1* and *RP1* were used as primers as described in Fig. 2b. The mutant background of *complementation lines* was identified by amplification using primers *LP2* and *LB*. Positive *ospk1-gc* lines were identified by amplification of the interrupted fragment using *LP1* and *RP1*. Positive *ospk1-cc* lines were identified by amplification of full-length CDS fragment using primers *CF* and *CR*. Rice genomic DNA was used as the template



roots and lateral roots (Fig. 5c). There was no GUS activity in the meristematic zone of lateral root tips (Fig. 5d). In the young floret, GUS expression was evident in glumes, anthers, stigma and style (Fig. 5e, f). Expression of GUS was also detected in milky stage seeds (Fig. 5g). Analysis of a cross section of the leaf blade revealed that strong GUS expression was localized in mesophyll cells (Fig. 5h). In the stem, GUS activity was mainly confined to phloem companion cells and some of the sclerenchyma cells in vascular bundles (Fig. 5i, j). In the root, GUS expression was restricted to the cortical parenchyma cells (Fig. 5k).

OsPK1 exhibits pyruvate kinase activity

OsPK1 encodes a putative protein with 527 amino acids. An orthologs search in the KEGG SSDB Database (<http://www.genome.jp/kegg/ssdb/>) showed that the top six orthologs are in *Zea mays*, *Sorghum bicolor*, *Vitis vinifera*, *Populus trichocarpa*, *Arabidopsis thaliana*, and *Ricinus communis* with sequence identity to *OsPK1* of 96, 95, 91, 90, 87 and 83%, respectively. The protein sequence alignment of *OsPK1* with Os12g0145700, umc2053, Sb05g002900 and AT2G36580 revealed their high

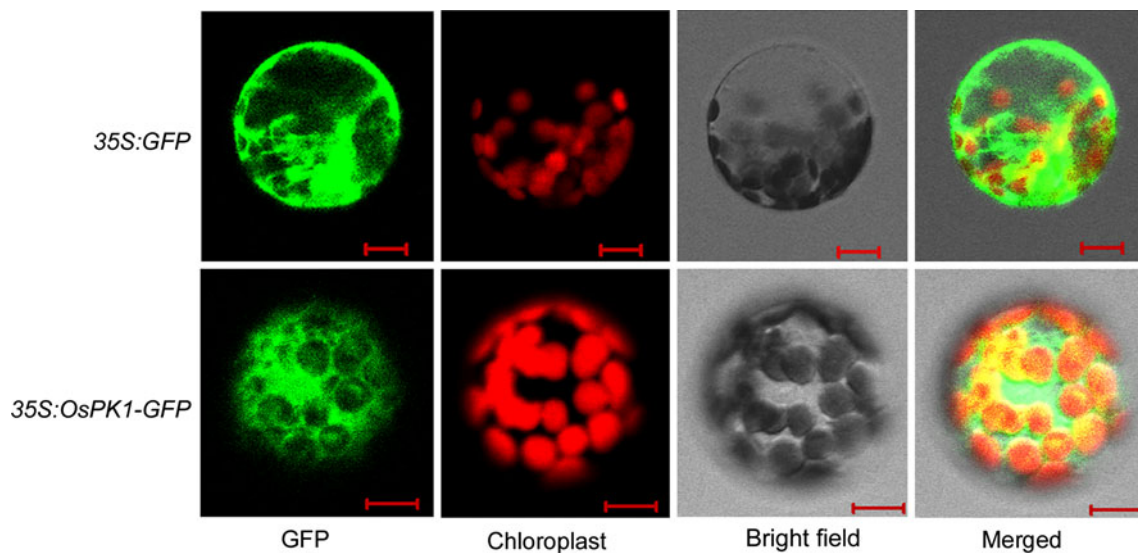


Fig. 4 Subcellular localization of OsPK1. *Arabidopsis* protoplast cells transiently expressing GFP alone (*top panel*) and OsPK1-GFP (*bottom panel*). Bars 10 μ m

homologies (Fig. 6a). Moreover, sequence searches in Pfam 24.0 (Finn et al. 2010; <http://pfam.sanger.ac.uk/>) showed that they all have the barrel domain (PF00224.14) and the alpha/beta domain (PF02887.9) of PK, implying that they all belong to the PK family.

To validate the PK activity of OsPK1, the intact OsPK1 was expressed in *E. coli* and purified under native conditions. The reaction containing purified OsPK1 showed a significant change in absorbance at 340 nm (A_{340}) within the first 5 min of the reaction (Fig. 6b). The A_{340} value did not change in the reaction omitting ADP. This confirmed that the change in the A_{340} value in the reaction containing purified OsPK1 is mainly due to its PK activity, rather than PEP phosphatase activity. Together, these results confirmed that OsPK1 has PK activity.

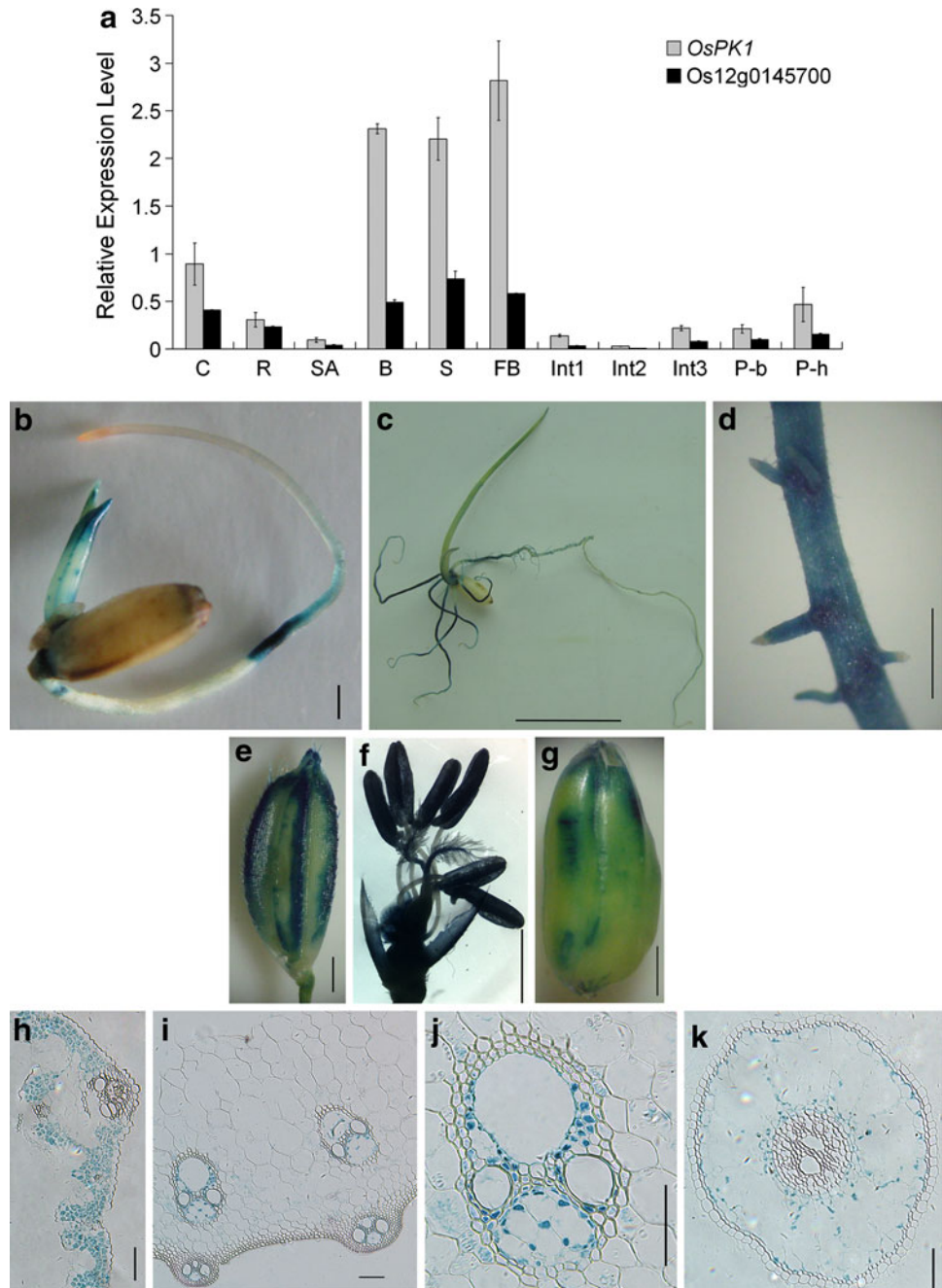
Since PK is a key enzyme of the glycolytic pathway, we analyzed the expression of four putative enzyme genes of glycolysis/gluconeogenesis pathway in 10-day-old seedlings of WT and *ospk1* (Fig. 6c). The expression of a putative triosephosphate isomerase (TIM) gene (Os09g0535000) was significantly increased in *ospk1*. TIM (EC:5.3.1.1) catalyzes the reversible interconversion of glyceraldehyde 3-phosphate and dihydroxyacetone phosphate. Expression of Os06g0256500, which encodes a putative glucose-6-phosphate isomerase (GPI), was also increased in *ospk1*. Expression of Os04g0119400, which encodes a putative pyruvate dehydrogenase (PDH), was decreased in *ospk1*. PDH converts pyruvate into acetyl CoA. This reaction is not part of glycolysis, but is the route of entry into the tricarboxylic acid (TCA) cycle in most organisms. In addition, *ospk1* showed increased expression

of Os01g0866400, which encodes a putative fructose-1, 6-bisphosphatase (FBPase), a critical regulatory enzyme in gluconeogenesis. These results suggest that the expression of certain enzyme genes of the glycolysis/gluconeogenesis pathway are interlinked in vivo, and are controlled by complex regulatory mechanisms.

Altered pyruvate/PEP metabolism in *ospk1*

The effects of the decreased expression of *OsPK1* on the pools of pyruvate and PEP in the third leaf blade of 10-day-old seedlings were analyzed (Fig. 7a). The amount of pyruvate is decreased in *ospk1*, and there is little difference in the amount of PEP between WT and *ospk1*, resulting in slightly decreased pyruvate/PEP ratio. The pyruvate and PEP data show that the decreased expression of *OsPK1* positively correlates with the pyruvate/PEP ratio due mostly to the effect on the steady-state level of pyruvate. The expression levels of the enzymes related to pyruvate/PEP metabolism, including malic enzyme (ME), PEP carboxykinase (PEPCK), PEP carboxylase (PEPC) and alanine transaminase (ALT) were examined by RT-PCR analysis (Fig. 7b). Compared with that in WT, lower level of *ME6* mRNA was detected in *ospk1*. *ME6* encodes a chloroplastic NADP-dependent ME. Os01g0208700, encoding a putative PEPC, was expressed increased in *ospk1*. The transcription levels of several isoforms of PK in WT and *ospk1* were also analyzed (Fig. 7c). Except for *OsPK1*, other isoforms showed no dramatic alterations, although a slightly increased level of Os07g0181000 and a slightly decreased level of Os10g0571200 were observed in *ospk1*.

Fig. 5 Expression pattern of *OsPK1*. **a** Quantitative RT-PCR analysis showing organ-specific expression of *OsPK1* and *Os12g0145700*. Transcription level was normalized to that of rice *Actin1* gene in different organs. *C* coleoptile, *R* young root, *SA* shoot apex of 2-week-old seedling, *B*, *S* the third leaf blade and leaf sheath of 2-week-old seedling, *FB* blade of flag leaf, *Int1-3* three internodes counted from top, *P-b* young panicle at booting stage, *P-h* panicle at heading stage. **b-k** GUS staining in various organs of *PRO_{OsPK1}::GUS* transgenic plants. **b** Young seedling after 3 days germination. **c** 7-day-old seedling with primary root, lateral roots, and adventitious roots. **d** Close view of lateral roots. **e** Young floret after heading stage. **f** Flower before pollination. **g** Milky stage seed. **h-k** Cross sections of mature leaf blade (**h**), stem (**i**) and root (**k**). **j** Enlargement of vascular bundle shown in **i**. Bars 1 mm (**b**, **d**, **e-g**), 1 cm (**c**) and 100 μ m (**h-k**)



Altered sugar metabolism and transport in *ospk1*

To determine whether carbohydrate metabolism and its transport to the sink tissues are disturbed in *ospk1* due to the decreased expression of *OsPK1*, sugar levels in WT and *ospk1* at the milky stage were measured by GC-MS analysis (Table 2). Compared with that of WT, the contents of glucose and fructose were markedly increased in flag leaf blade and panicle of *ospk1*. The contents of glucose, fructose, galactose, and sucrose in Int2 (the second internode counted from top) were all decreased in *ospk1*. The

content of sucrose in panicle of *ospk1* was decreased by approximately 84%. These findings indicated that both monosaccharide metabolism and sugar transport are altered in *ospk1*.

Discussion

Although there have been a number of physiological and biochemical studies on PK_c in plants, its role has not yet been fully elucidated. In this study, we provide evidence

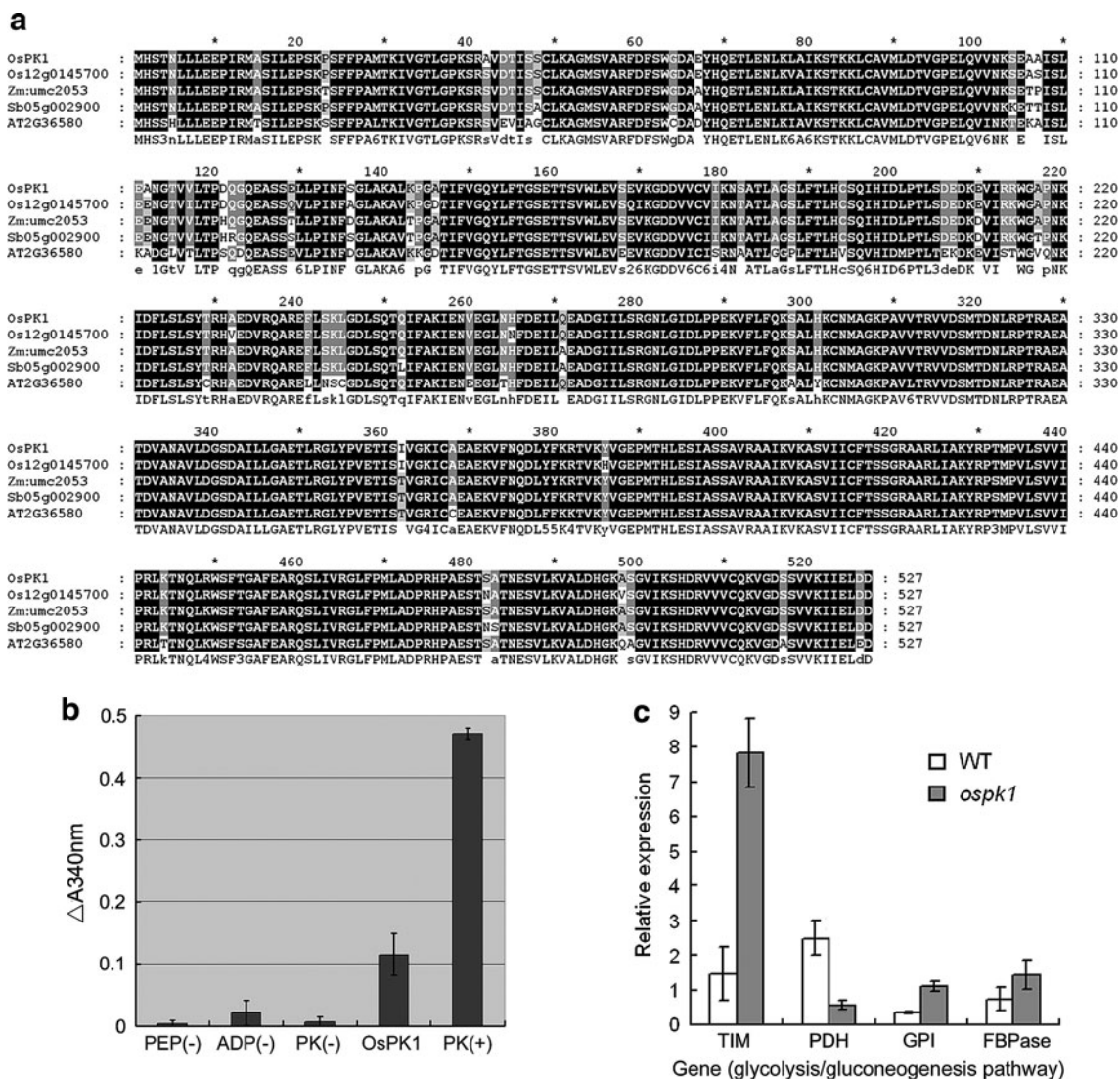


Fig. 6 Determination of pyruvate kinase activity of OsPK1. **a** Protein sequence alignment of OsPK1 and its homologs using GeneDoc. Os, *Oryza sativa*; Zm, *Zea mays*; Sb, *Sorghum bicolor*; AT, *Arabidopsis thaliana*. Two significant Pfam matches, barrel domain and alpha/beta domain of pyruvate kinase, are located at positions 28–380 and 394–524, respectively. Conserved amino acids are highlighted in black and gray: white letter with black background (100% identity); white letter with gray background (80%); black letter with gray background (60%). **b** Enzymatic activity was determined spectrophotometrically by measuring the change in absorbance at 340 nm (A_{340} value at 5 min subtracted from that at 0 min). OsPK1, expressed in *E.coli* and purified under native conditions. PEP(–), ADP(–) and

that a PK_c isozyme of rice, designated as OsPK1, is critical for rice morphological development. Pyruvate kinase phylogeny analysis revealed that OsPK1 has very close orthologs in other cereal crops (Fig. S2). OsPK1 displays very high amino acid sequence identity with its orthologs from *Zea mays*, *Sorghum bicolor* and *Arabidopsis thaliana* (Fig. 6a). These findings imply that this protein and its orthologs may play a basic role in the normal growth and

PK(–), negative controls, PEP, ADP, and PK, respectively, were omitted from the reaction. PK(+), positive control, pyruvate kinase from rabbit muscle. Values are mean ± SD from three independent experiments. **c** Altered expression of putative enzyme genes of glycolysis/gluconeogenesis pathway in *ospk1*. Gene expression was normalized to that of rice *Actin1* gene. RNA used for quantitative RT-PCR analysis was isolated from the third leaf blade of 10-day-old seedlings. TIM, Os09g0535000, noted as triosephosphate isomerase; PDH, Os04g0119400, noted as pyruvate dehydrogenase; GPI, Os06g0256500, noted as glucose-6-phosphate isomerase; FBPase, Os01g0866400, noted as fructose-1,6-bisphosphatase

development of plants, although they became two branches after the separation of monocots and dicots.

Previous studies in vascular plants revealed that PK exists as tissue-specific isozymes (Plaxton and Podesta 2006). The expression pattern of *OsPK1* showed a surprising degree of specificity and complexity. First, *OsPK1* expression was higher in functional green leaves than in unexpanded leaves (Fig. 5a). Second, in roots, GUS

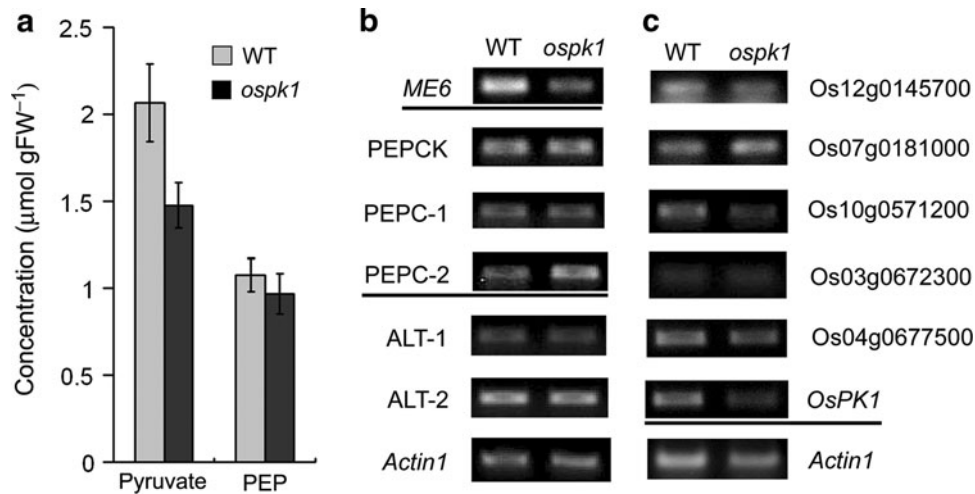


Fig. 7 The metabolism of pyruvate and PEP in WT and *ospk1*. The third leaf blade of 10-day-old seedlings was used for the analysis. **a** Pyruvate and PEP contents in WT and *ospk1*. Two biological replications were performed in each experiment. Values are mean \pm SD from three independent experiments. **b** RT-PCR analysis of genes related to pyruvate/PEP metabolism. *ME6*, Os01g0188400,

chloroplastic NADP-dependent malic enzyme; *PEPCK*, Os10g0204400, noted as PEP carboxykinase; *PEPC*, PEP carboxylase; *PEPC-1*, Os02g0244700; *PEPC-2*, Os01g0208700; *ALT*, alanine transaminase; *ALT-1*, Os10g0390500; *ALT-2*, Os07g0108300. **c** RT-PCR analysis of genes encoding putative PK. In **b** and **c**, the rice *Actin1* gene was used as a reference of RNA concentration

Table 2 Sugar levels in WT and *ospk1* at the milky stage

	Glucose ($\mu\text{g g FW}^{-1}$)	Fructose ($\mu\text{g g FW}^{-1}$)	Galactose ($\mu\text{g g FW}^{-1}$)	Sucrose ($\mu\text{g g FW}^{-1}$)
WT-FB	379 \pm 22	214 \pm 10	50 \pm 5	3,434 \pm 520
<i>ospk1</i> -FB	656 \pm 14	347 \pm 12	65 \pm 3	3,668 \pm 335
WT-Int2	861 \pm 165	574 \pm 18	131 \pm 20	15,100 \pm 2,453
<i>ospk1</i> -Int2	283 \pm 9	129 \pm 6	41 \pm 2	12,628 \pm 153
WT-panicle	878 \pm 92	485 \pm 85	168 \pm 17	3,435 \pm 15
<i>ospk1</i> -panicle	1,602 \pm 114	1,367 \pm 218	209 \pm 58	534 \pm 7

Two biological replications were performed in each experiment. Values are mean \pm SD from three independent experiments
FB flag leaf blade, *Int2* the second internode counted from top

staining was detected mainly in the maturation zone or root-hair zone of the root tip (Fig. 5b–d). Furthermore, GUS expression was stronger in adventitious roots than in the primary root. Absorption of water and nutrients in rice is mainly performed by the maturation zone of primary root and subsequently by root-hair zone of adventitious roots. These findings indicated that *OsPK1* expression in roots is confined to the execution sites of absorption. Third, at the cellular level, *OsPK1* transcripts were localized in mesophyll cells in leaves, phloem companion cells and some of the sclerenchyma cells in vascular bundles in stems, and in cortical parenchyma cells in roots (Fig. 5h–k). It is noteworthy that the companion cell is more metabolically active than a ‘typical’ plant cell. It has more ribosomes and mitochondria than a ‘typical’ cell, and the survival of sieve-tube members depends on their close association with the companion cells. Thus, *OsPK1* appears to be expressed predominately in these functional tissues and

cell types, implying that *OsPK1*, as a PK_c isozyme, is critical for diverse metabolic processes in rice, including the metabolism in leaves, the assimilate transport through stems, and exogenous nutrient uptake by roots.

The dynamic and complicated expression of *OsPK1* according to the diverse developmental demands must be under fine regulation, especially at the transcriptional level. In the *ospk1* mutant, analysis of the flanking sequences revealed that a T-DNA integration occurred at nucleotide position –120 upstream of the transcription initiation site, which was accompanied by a 29-bp deletion of rice genomic DNA (from nt –121 to –149). *OsPK1* expression was decreased by approximately 90% in the root, leaf, internode and panicle of *ospk1* compared with that in WT (Fig. 2c). Therefore, we can speculate that a *cis*-element is located around position –120, and that this element binds a ubiquitous activator. The sequence alignment results suggested that Os12g0145700 does not have similar putative *cis*-element.

In the *ospk1* mutant, 'sh'-type dwarfism, panicle enclosure and reduced seed set are three sequential defective phenotypes. The UI length of *ospk1* is reduced to 26.7% of that of WT. The shortened UI is unable to push the panicle completely out of the flag leaf sheath, resulting in serious panicle enclosure. The majority of the panicle is enclosed within the flag leaf sheath, which blocks normal pollination and leads to greatly reduced seed production (Yin et al. 2007). Consistent with this, *ospk1* showed greatly reduced seed set (Table 1).

The decreased expression of *OsPK1* affected the expression of putative enzyme genes of the glycolysis/gluconeogenesis pathway in *ospk1* (Fig. 6c). Therefore, *OsPK1* may function through the glycolytic pathway as a key regulatory enzyme. The glycolytic pathway produces important precursor metabolites, some of which can be imported into the plastid. For example, PEP is imported into plastids of *B. napus* embryos (Kubis et al. 2004). Expression of Os09g0535000, which is similar to the chloroplast precursor of TIM, was markedly increased in *ospk1* (fivefold compared with that in WT), implying that there are significant changes in sugar metabolism in the mutant chloroplast.

There are three ways in which carbon can enter the TCA cycle (Jenner et al. 2001). First, PEP produced in glycolysis can be converted into pyruvate, and subsequently PDH complex converts pyruvate into acetyl CoA for direct entry into the mitochondria. Second, PEP can be carboxylated by PEPC to oxaloacetate (OAA), which can also enter the mitochondria (Ebbighausen et al. 1985; Kromer et al. 1996). Third, OAA can be reduced in the cytosol and the malate produced can enter the mitochondria. Thus, malate and OAA supplement mitochondrial pools of C₄ acids to fulfill an anaplerotic role. The amount of pyruvate is decreased in *ospk1* (Fig. 7a), and expression of Os04g0119400, which encodes a putative PDH, was decreased in *ospk1* (Fig. 6c), implying that the first way entering the TCA cycle is impaired in *ospk1*. Os01g0208700, encoding a putative PEPC, was expressed increased in *ospk1* (Fig. 7b). It is possible that the second way entering the TCA cycle is enhanced in *ospk1* due to increased PEPC expression in the anaplerotic pathway. Non-photosynthetic isoforms of NADP-ME were found in the cytosol and plastids of some C₃ plants (Drincovich et al. 2001). The decreased transcription level of *ME6* in *ospk1* implied that malate partitioning was altered in *ospk1*.

Measurement of sugars revealed that transgenic tubers with decreased PK_c had significantly higher level of glucose and sucrose (Oliver et al. 2008). Here, the contents of glucose and fructose accumulated abundantly in flag leaf blade and panicle of *ospk1*. It is reasonable that an inhibition of glycolytic flux and an accumulation of carbohydrate precursors caused by the decreased expression of

OsPK1. Compared with that in WT, the sugar contents detected in Int2 were all decreased in *ospk1*. Moreover, the level of sucrose in panicle was decreased in *ospk1*. These findings suggested that the carbohydrate transport to sink tissues was disturbed. Companion cells have a critical role in the transport of sugars and amino acids into and out of the sieve elements. It is speculated that the decreased expression of *OsPK1* in phloem companion cells of stem in *ospk1* could reduce the sugar transport efficiency. In most higher plants, sucrose is the main transport form for carbon partitioning between source and sink tissue via the phloem (Van Bel 2003). Whether sucrose or monosaccharides are delivered influences plant development greatly, as could be demonstrated for the seed development (Borisjuk et al. 2004). The distinctly decreased sucrose level in panicle of *ospk1* could be one of the reasons for shrunken grains and low seed set.

It has been demonstrated that PK_c in tobacco leaves and castor leaves is a heterotetramer consisting of two subunits of 57 and 56 kDa (Plaxton 1989; Knowles et al. 1998). And it has been described that the presence of the 49-kDa subunit is required to maintain stability of the 52-kDa subunit in the heterotetrameric plant AGPase (Wang et al. 1998). It is speculated that *OsPK1*, as a PK subunit, is coordinated with the other subunit to fulfill its role. Maybe it makes easier to understand that just decreased expression of *OsPK1* has such drastic impacts on the growth and development of rice, but it requires reliable evidence. Further research underway in our laboratory is aimed at determining how expression of *OsPK1* is regulated, and how *OsPK1* and its potential partners (other PKs) are coordinated to regulate the glycolytic pathway.

Acknowledgments We thank Xiangning Jiang and Xiaoqiao Cheng of Beijing Forestry University for technical assistance for sugar measurement. This work was supported by grants from the National Natural Science Foundation of China (Grant No. 30571003) and the Natural Science Foundation of Hainan Province (Grant No. 30204).

References

- Andre C, Froehlich JE, Moll MR, Benning C (2007) A heteromeric plastidic pyruvate kinase complex involved in seed oil biosynthesis in *Arabidopsis*. *Plant Cell* 19:2006–2022
- Arabidopsis Genome Initiative (2000) Analysis of the genome sequence of the flowering plant *Arabidopsis thaliana*. *Nature* 408:796–815
- Baud S, WUILLEME S, Dubreucq B, de Almeida A, Vuagnat C, Lepiniec L, Miquel M, Rochat C (2007) Function of plastidial pyruvate kinases in seeds of *Arabidopsis thaliana*. *Plant J* 52:405–419
- Borisjuk L, Rolletschek H, Radchuk R, Weschke W, Wobus U, Weber H (2004) Seed development and differentiation: a role for metabolic regulation. *Plant Biol* 6:375–386

- Cole KP, Blakeley SD, Dennis DT (1992) Structure of the gene encoding potato cytosolic pyruvate-kinase. *Gene* 122:255–261
- Dai MQ, Zhao Y, Ma Q, Hu YF, Hedden P, Zhang QF, Zhou DX (2007) The rice *YABBY1* gene is involved in the feedback regulation of gibberellin metabolism. *Plant Physiol* 144:121–133
- Drincovich MF, Casati P, Andreo CS (2001) NADP-malic enzyme from plants: a ubiquitous enzyme involved in different metabolic pathways. *FEBS Lett* 490:1–6
- Ebbighausen H, Chen J, Heldt HW (1985) Oxaloacetate translocator in plant mitochondria. *Biochim Biophys Acta* 810:184–199
- Finn RD, Mistry J, Tate J, Coghill P, Heger A, Pollington JE, Gavin OL, Guneseakaran P, Ceric G, Forslund K, Holm L, Sonnhammer EL, Eddy SR, Bateman A (2010) The Pfam protein families database. *Nucl Acids Res* 38:D211–D222
- Grodzinski B, Jiao J, Knowles VL, Plaxton WC (1999) Photosynthesis and carbon partitioning in transgenic tobacco plants deficient in leaf cytosolic pyruvate kinase. *Plant Physiol* 120:887–895
- Hausler RE, Fischer KL, Flugge UI (2000) Determination of low-abundant metabolites in plant extracts by NAD(P)H fluorescence with a microtiter plate reader. *Anal Biochem* 281:1–8
- Hiei Y, Ohta S, Komari T, Kumashiro T (1994) Efficient transformation of rice (*Oryza sativa* L.) mediated by *Agrobacterium* and sequence analysis of the boundaries of the T-DNA. *Plant J* 6:271–282
- Hu ZY, Plaxton WC (1996) Purification and characterization of cytosolic pyruvate kinase from leaves of the castor oil plant. *Arch Biochem Biophys* 333:298–307
- Jenner HL, Winning BM, Millar AH, Tomlinson KL, Leaver CJ, Hill SA (2001) NAD malic enzyme and the control of carbohydrate metabolism in potato tubers. *Plant Physiol* 126:1139–1149
- Kayne FJ, Price NC (1973) Amino acid effector binding to rabbit muscle pyruvate kinase. *Arch Biochem Biophys* 159:292–296
- Knowles VL, McHugh SG, Hu ZY, Dennis DT, Miki BL, Plaxton WC (1998) Altered growth of transgenic tobacco lacking leaf cytosolic pyruvate kinase. *Plant Physiol* 116:45–51
- Kromer S, Gardestrom P, Samuelsson G (1996) Regulation of the supply of cytosolic oxaloacetate for mitochondrial metabolism via phosphoenolpyruvate carboxylase in barley leaf protoplasts: I. The effect of covalent modification on PEPC activity, pH response, and kinetic properties. *Biochim Biophys Acta* 1289:343–350
- Kubis SE, Pike MJ, Hill LM, Rawsthorne S (2004) The import of phosphoenolpyruvate by plastids from developing embryos of oilseed rape *Brassica napus* (L.), and its potential as a substrate for fatty acid synthesis. *J Exp Bot* 55:1455–1462
- Li XY, Qian Q, Fu ZM, Wang YH, Xiong GS, Zeng DL, Wang XQ, Liu XF, Teng S, Hiroshi F, Yuan M, Luo D, Han B, Li JY (2003) Control of tillering in rice. *Nature* 422:618–621
- Li XY, Lin HQ, Zhang WG, Zou Y, Zhang J, Tang XY, Zhou JM (2005) Flagellin induces innate immunity in nonhost interactions that is suppressed by *Pseudomonas syringae* effectors. *Proc Natl Acad Sci USA* 102:12990–12995
- Liu YG, Mitsukawa N, Oosumi T, Whittier RF (1995) Efficient isolation and mapping of *Arabidopsis thaliana* T-DNA insert junctions by thermal asymmetric interlaced PCR. *Plant J* 8:457–463
- Malcovati M, Valentini G, Kornberg HL (1973) Two forms of pyruvate kinase in *E. coli*: their properties and regulation. *Acta Vitaminol Enzymol* 27:96–111
- McHugh SG, Knowles VL, Blakeley SD, Sangwan RS, Miki BL, Dennis DT, Plaxton WC (1995) Differential expression of cytosolic and plastid pyruvate kinase isozymes in tobacco. *Physiol Plant* 95:507–514
- Munoz ME, Ponce E (2003) Pyruvate kinase: current status of regulatory and functional properties. *Comp Biochem Physiol B Biochem Mol Biol* 135:197–218
- Oliver SN, Lunn JE, Urbanczyk-Wochniak E, Lytovchenko A, van Dongen JT, Faix B, Schmalzlin E, Fernie AR, Geigenberger P (2008) Decreased expression of cytosolic pyruvate kinase in potato tubers leads to a decline in pyruvate resulting in an in vivo repression of the alternative oxidase. *Plant Physiol* 148:1640–1654
- Plaxton WC (1989) Molecular and immunological characterization of plastid and cytosolic pyruvate kinase isoenzymes from castor-oil-plant endosperm and leaf. *Eur J Biochem* 181:443–451
- Plaxton WC (1996) The organization and regulation of plant glycolysis. *Annu Rev Plant Physiol Plant Mol Biol* 47:185–214
- Plaxton WC, Podesta FE (2006) The functional organization and control of plant respiration. *Crit Rev Plant Sci* 25:159–198
- Plaxton WC, Smith CR, Knowles VL (2002) Molecular and regulatory properties of leucoplast pyruvate kinase from *Brassica napus* (rapeseed) suspension cells. *Arch Biochem Biophys* 400:54–62
- Sha Y, Li S, Pei Z, Luo L, Tian Y, He C (2004) Generation and flanking sequence analysis of a rice T-DNA tagged population. *Theor Appl Genet* 108:306–314
- Tan YP, Li K, Hu L, Chen S, Gai Y, Jiang XN (2010) Fast and simple droplet sampling of sap from plant tissues and capillary microextraction of soluble saccharides for picogram-scale quantitative determination with GC–MS. *J Agric Food Chem* 58:9931–9935
- Tang GQ, Hardin SC, Dewey R, Huber SC (2003) A novel C-terminal proteolytic processing of cytosolic pyruvate kinase, its phosphorylation and degradation by the proteasome in developing soybean seeds. *Plant J* 34:77–93
- Turner WL, Plaxton WC (2000) Purification and characterization of cytosolic pyruvate kinase from banana fruit. *Biochem J* 352:875–882
- Turner WL, Knowles VL, Plaxton WC (2005) Cytosolic pyruvate kinase: subunit composition, activity, and amount in developing castor and soybean seeds, and biochemical characterization of the purified castor seed enzyme. *Planta* 222:1051–1062
- Van Bel AJE (2003) The phloem, a miracle of ingenuity. *Plant Cell Environ* 26:125–149
- Wang SM, Lue WL, Yu TS, Long JH, Wang CN, Eimert K, Chen J (1998) Characterization of *ADGL1*, an *Arabidopsis* locus encoding for ADPG pyrophosphorylase small subunit, demonstrates that the presence of the small subunit is required for large subunit stability. *Plant J* 13:63–70
- Yamada K, Noguchi T (1999) Nutrient and hormonal regulation of pyruvate kinase gene expression. *Biochem J* 337:1–11
- Yamamuro C, Ihara Y, Wu X, Noguchi T, Fujioka S, Takatsuto S, Ashikari M, Kitano H, Matsuoka M (2000) Loss of function of a rice *brassinosteroid insensitive1* homolog prevents internode elongation and bending of the lamina joint. *Plant Cell* 12:1591–1605
- Yin CX, Gan LJ, Ng D, Zhou X, Xia K (2007) Decreased panicle-derived indole-3-acetic acid reduces gibberellin A₁ level in the uppermost internode, causing panicle enclosure in male sterile rice Zhenshan 97A. *J Exp Bot* 58:2441–2449